

Experimental demonstration of free-space information transfer using phase modulated orbital angular momentum radio

F. Tamburini,^{1, a)} B. Thidé,^{2, b)} V. Boaga,³ F. Carraro,^{3, c)} M. del Pup,³ A. Bianchini,⁴ C.G. Smeda,⁵ and F. Romanato^{6, d)}

¹⁾*Twist-Off srl, via Croce Rossa 112, IT-35129 Padova, Italy, EU*

²⁾*Swedish Institute of Space Physics, Ångström Laboratory, P. O. Box 537, SE-75121 Uppsala, Sweden, EU*

³⁾*ARI, Sezione Venezia, Santa Croce 1996, IT-30123 Venice, Italy, EU*

⁴⁾*Department of Physics and Astronomy, University of Padova, vicolo dell'Osservatorio 3, IT-35122 Padova, Italy, EU*

⁵⁾*GHT Photonics srl, via Istria 55, IT-35135 Padova, Italy, EU*

⁶⁾*Department of Physics and Astronomy, University of Padova, via Marzolo 8, IT-35131 Padova, Italy, EU*

(Dated: 2013-02-14 13:04:38Z)

In a series of fundamental proof-of-principle studies, including numerical, controlled indoor laboratory, and real-world outdoor experiments, we have shown that it is possible to use electromagnetic angular momentum as a physical layer for radio science and radio communication applications^{1–5}. Here we report a major, decisive step toward the realization of the latter, in the form of a real-world experimental demonstration that a radio beam carrying orbital angular momentum (OAM) can readily be digitally phase shift modulated and that the information thus encoded can be effectively transferred in free space to a remote receiver. The experiment was carried out in an urban setting and showed that the information transfer is robust against ground reflections and interfering radio signals. The importance of our results lies in the fact that digital phase shift keying (PSK) protocols are used in many present-day wireless communication scenarios, allowing new angular momentum radio implementations to use methods and protocols that are backward compatible with existing linear momentum ones.

I. INTRODUCTION

Current radio science and communication implementations based on the electromagnetic (EM) linear momentum (Poynting vector) physics layer are beginning to approach their limits in terms of radio frequency spectrum availability and occupancy. This calls for the introduction of new radio paradigms. For this purpose, it has been proposed that the EM angular momentum, well described in the standard literature^{6–21} but hitherto underutilized in radio science and technology, be fully exploited in radio communications^{1–5,22,23}. As has been amply demonstrated in experiments at optical frequencies, the use of EM angular momentum can indeed increase the information entropy and hence the capacity of wireless communications^{24–30}. This is consistent with the fact that all classical fields carry angular momentum^{31,32} and that the dynamics of a general physical system is not fully described unless both its total linear momentum and total angular momentum are specified³³. Specifying only one of them is not sufficient. And not using both the linear and the angular momentum of an EM field is therefore not using the field to its full capacity.

In order to add information transfer capacity to present-day radio communication links, it is common practice to invoke EM spin angular momentum (SAM) in the form of wave polarization. SAM is an intrinsic property of the classical EM

field (and each individual photon), describing the spin characteristics of the EM rotational degrees of freedom. However, in free space SAM can attain only two values, $\sigma = \pm 1$, corresponding to left-hand and right-hand wave polarization, respectively. In other words, SAM spans a two-dimensional state space (Hilbert space). By invoking SAM one can therefore, at most, double the information transfer capacity within a given frequency bandwidth. The physical encoding of a beam with SAM causes the EM field phases of the beam to be different in *different directions at one and the same point* in a plane perpendicular to the beam axis. A common technique to demonstrate and exploit SAM in radio is to use two co-located orthogonal dipole antennas, also known as turnstile antennas. Another common technique is to use helical antennas.

In contrast, the EM orbital angular momentum (OAM) is an extrinsic property of the EM field (and each individual photon), describing the orbital characteristics of its rotational degrees of freedom. Associated with OAM is an EM field phase factor $\exp\{i\alpha\varphi\}$ where φ is the azimuthal angle around the beam axis. Of course, the phase function α may attain any value, not necessarily only integers. However, due to the single-valuedness of the fields, OAM is quantized such that an EM field that carries non-integer OAM is a weighted superposition of discrete OAM eigenmode components, each of which is proportional to $\exp\{\pm im\varphi\}$, where $m = 0, 1, 2, \dots$, acts as a quantum number^{3,34}, also called the topological charge.

Hence, a beam carrying an arbitrary amount of OAM contains a spectrum of discrete integer OAM eigenmodes³⁵ that are mutually orthogonal (in a function space sense) and therefore propagate independently³⁶. In other words, OAM spans a state space of dimensionality $N = 1, 2, 3, \dots$, and can therefore be regarded as an ‘azimuthal polarization’ with arbitrarily many states³⁷. This makes it possible, at least in principle, to use OAM to physically encode an unlimited amount of inform-

^{a)}Also at: ARI, Sezione Venezia, Santa Croce 1996, IT-30123 Venice, Italy, EU

^{b)}E-mail: bt@ifu.se

^{c)}Also at: Ro.ver Instruments, via Parini 2, IT-25019 Sirmione (VR), Italy, EU

^{d)}Also at: LaNN Venetonanotech, via Stati Uniti 4, IT-35100 Padova, Italy, EU

Table I. Similarities and differences between the EM linear momentum density $\mathbf{g}^{\text{field}}(t, \mathbf{x})$ and the EM angular momentum density $\mathbf{h}^{\text{field}}(t, \mathbf{x}, \mathbf{x}_0)$ around a moment point \mathbf{x}_0 carried by a classical electromagnetic field $[\mathbf{E}(t, \mathbf{x}), \mathbf{B}(t, \mathbf{x})]$ in the presence of matter (particles) with mechanical linear momentum density $\mathbf{g}^{\text{mech}}(t, \mathbf{x})$ and mechanical angular momentum density $\mathbf{h}^{\text{mech}}(t, \mathbf{x}, \mathbf{x}_0)$.

Property	Linear momentum density	Angular momentum density
Definition	$\mathbf{g}^{\text{field}} = \epsilon_0 \mathbf{E} \times \mathbf{B}$	$\mathbf{h}^{\text{field}} = (\mathbf{x} - \mathbf{x}_0) \times (\epsilon_0 \mathbf{E} \times \mathbf{B})$
SI unit	$\text{N s m}^{-3} (\text{kg m}^{-2} \text{s}^{-1})$	$\text{N s m}^{-2} (\text{kg m}^{-1} \text{s}^{-1})$
Spatial fall off at large distances r	$\sim r^{-2} + \mathcal{O}(r^{-3})$	$\sim r^{-2} + \mathcal{O}(r^{-3})$
Typical phase factor	$\exp\{i(\mathbf{k} \cdot \mathbf{x} - \omega t)\}$	$\exp\{i(\mathbf{k} \cdot \mathbf{x} - \omega t + \alpha \varphi)\}, 0 \leq \varphi < 2\pi$
Local conservation law	$\frac{\partial \mathbf{g}^{\text{mech}}}{\partial t} + \frac{\partial \mathbf{g}^{\text{field}}}{\partial t} + \nabla \cdot \mathbf{T} = \mathbf{0}$	$\frac{\partial \mathbf{h}^{\text{mech}}}{\partial t} + \frac{\partial \mathbf{h}^{\text{field}}}{\partial t} + \nabla \cdot \mathbf{K} = \mathbf{0}$
C (charge conjugation) symmetry	Even	Even
P (spatial inversion) symmetry	Even (polar vector, ordinary vector)	Odd (axial vector, pseudovector)
T (time reversal) symmetry	Odd	Odd

ation onto any part of an EM beam, down to the individual photon³⁸. The physical encoding of a beam with OAM causes the EM field of the beam to attain a whole set of unique characteristics. One of these characteristics is that the EM field exhibits different phases when measured in *one and the same direction at different points* in a plane perpendicular to the beam axis. In our experiments we can therefore use standard phase interferometers constructed from ordinary (linear momentum) antennas to analyze the OAM content of the beams.

It should be emphasized that for EM beams of the kind used in the experiment described here, OAM is distinctively different from—and independent of—SAM (wave polarization). If such a beam is already N -fold OAM encoded, adding SAM will double the information transfer capacity by virtue of the fact that the dimensionality of the state space doubles from N to $2N$. So far we have not utilized the polarization (SAM) degree of freedom in our OAM radio experiments. Such experiments are pending.

Proof-of-concept studies have shown that it is possible to use the total angular momentum, *i.e.* SAM+OAM, as a new physical layer for radio science and technology exploitation. These studies include numerical experiments¹ showing that it is feasible to utilize OAM in radio; controlled anechoic chamber laboratory experiments³ verifying that it is possible to generate and transmit radio beams carrying non-integer OAM and to measure their OAM spectra in the form of weighted superpositions of different integer OAM eigenstates; and outdoor experiments⁴ verifying that in a real-world setting different signals, encoded in different OAM states, can be transmitted independently to a receiver located in the (linear momentum) far zone and be resolved there.

We have therefore proposed that the angular momentum physical layer be used as an alternative and/or supplement to the linear momentum (Poynting vector) physical layer that is used in current radio communication implementations. As an important step in the practical implementation of this, we recently demonstrated experimentally that information encoded in OAM radio beams in terms of quadrature phase shift coding (QPSK) modulation can be robustly transferred in free space even in the presence of reflections and interfering radio signals. The results of this experiment are presented here.

II. PHYSICAL BACKGROUND

Let $\mathbf{g}^{\text{field}}$ and $\mathbf{h}^{\text{field}}$ denote the volumetric EM linear and angular momenta densities, respectively, some properties of which are listed in Table I. Then the total classical EM linear momentum, localized inside a volume V in free space where the dielectric permittivity is ϵ_0 , is given by^{14,17,23}

$$\begin{aligned} \mathbf{p}^{\text{field}}(t) &= \int_V d^3x \mathbf{g}^{\text{field}}(t, \mathbf{x}) \\ &= \epsilon_0 \int_V d^3x [\mathbf{E}(t, \mathbf{x}) \times \mathbf{B}(t, \mathbf{x})] \end{aligned} \quad (1a)$$

and the total classical EM angular momentum (SAM+OAM) around an arbitrary moment point \mathbf{x}_0 carried by the same EM field in this volume V is given by^{14,17,23}

$$\begin{aligned} \mathbf{J}^{\text{field}}(t, \mathbf{x}_0) &= \int_V d^3x \mathbf{h}^{\text{field}}(t, \mathbf{x}, \mathbf{x}_0) \\ &= \int_V d^3x (\mathbf{x} - \mathbf{x}_0) \times \mathbf{g}^{\text{field}}(t, \mathbf{x}) \\ &= \epsilon_0 \int_V d^3x (\mathbf{x} - \mathbf{x}_0) \times [\mathbf{E}(t, \mathbf{x}) \times \mathbf{B}(t, \mathbf{x})] \\ &= \mathbf{J}^{\text{field}}(t, \mathbf{0}) - \mathbf{x}_0 \mathbf{p}^{\text{field}}(t) \end{aligned} \quad (1b)$$

For a localized source, it is convenient to evaluate the integrals in eqns. (1) in a spherical polar coordinate system (r, θ, φ) with its origin at the barycentre of the source region. A signal pulse emitted by the source during a finite time interval Δt , will, after it has left the source region, be propagating radially outward, in the surrounding free space, with speed c and be confined to a finite volume V_0 between two spherical shells, one with radius r_0 relative to the source, and another with radius $r_0 + \Delta r_0$ where $\Delta r_0 = c\Delta t$ and with a certain distribution in the angular (θ, φ) domain¹⁴. Consequently, the total linear momentum carried by such an EM pulse propagating in free space is

$$\begin{aligned} &\int_{V_0} d^3x_0 \mathbf{g}^{\text{field}}(t, \mathbf{x}) \\ &= \int_{r_0}^{r_0 + \Delta r_0} dr r^2 \int_0^{2\pi} d\varphi \int_0^\pi d\theta \sin \theta \mathbf{g}^{\text{field}}(t, r, \theta, \varphi) \end{aligned} \quad (2)$$

Integration of $\mathbf{g}^{\text{field}}$ over the angular domain [the two last integrals in eqn. (2)] yields a function of r (and t) that, for very large r_0 , becomes proportional to r^{-2} ; cf. Table I and Refs. 5, 39, and 40). Taking into account that this function shall in the remaining integral in eqn. (2) be multiplied by r^2 and then integrated over a finite radial interval $[r_0, r_0 + \Delta r_0]$, the entire integral, and hence $\mathbf{p}^{\text{field}}$, tends to a constant when r_0 tends to infinity. This asymptotic independence of r , allowing the EM linear momentum generated by a localized source to be transported all the way to infinity without radial fall off and therefore be irreversibly lost from the source, is the famous arrow of radiation asymmetry (see Ref. 41, pp. 328–329, and Ref. 42, Chap. 6).

Recalling the fact that the angular momentum density $\mathbf{h}^{\text{field}}$ has precisely the same asymptotic r^{-2} radial fall off as the linear momentum density $\mathbf{g}^{\text{field}}$ (see Table I, and Refs. 5, 39, and 40), it is clear that also the emitted angular momentum tends asymptotically to a constant at very large distances from the source and is irreversibly lost there. This is the angular momentum analogue of the above mentioned linear momentum arrow of radiation.

Consequently, both linear and angular momenta can propagate—and be used for information transfer—over, in principle, arbitrarily long distances. Of course, the magnitude and angular distribution of the respective momentum densities depend on the specific spatio-temporal and topological EM properties of the actual radiating device used. Some devices, such as the linear antennas used in radio today, are effective radiators and sensors of linear momentum whereas angular momentum is more optimally radiated and sensed by other devices. In radio engineering parlance, the angular distribution of the linear momentum density (Poynting vector) is often referred to as the ‘radiation pattern’ or ‘antenna diagram’. It should be noted that for one and the same radiating system this angular distribution of the *linear* momentum density (‘radiation pattern’) is *not* the same as the angular distribution of the *angular* momentum density. See Refs. 21 and 43.

As shown by well-known conservation laws that follow directly from Maxwell’s equations, the two physical observables total linear momentum and total angular momentum are conserved (constants of motion). Hence, $\mathbf{p}^{\text{field}}$ and $\mathbf{J}^{\text{field}}$ in a fixed volume an EM beam propagating in free space can neither decrease nor increase.

We recall that the linear momentum fulfils the conservation law^{14,15,21}

$$\frac{d\mathbf{p}^{\text{field}}}{dt} + \mathbf{F} + \oint_S d^2x \hat{\mathbf{n}} \cdot \mathbf{T} = \mathbf{0} \quad (3a)$$

where \mathbf{T} is the EM linear momentum flux tensor (the negative of Maxwell’s stress tensor), and

$$\mathbf{F} = \frac{d\mathbf{p}^{\text{mech}}}{dt} \quad (3b)$$

is the mechanical force (Newton’s second law, Euler’s first law) on the particles (\mathbf{p}^{mech} being the mechanical momentum),

The angular momentum fulfils the conservation law^{14,15,21}

$$\frac{d\mathbf{J}^{\text{field}}(\mathbf{x}_0)}{dt} + \boldsymbol{\tau}(\mathbf{x}_0) + \oint_S d^2x \hat{\mathbf{n}} \cdot \mathbf{K}(\mathbf{x}_0) = \mathbf{0} \quad (4a)$$

where \mathbf{K} is the EM angular momentum flux tensor and

$$\boldsymbol{\tau}(\mathbf{x}_0) = \frac{d\mathbf{J}^{\text{mech}}(\mathbf{x}_0)}{dt} \quad (4b)$$

is the mechanical torque (Euler’s second law) on the particles (\mathbf{J}^{mech} being the mechanical angular momentum).

Eqns. (4) clearly show that angular-momentum radio beams should ideally be radiated and sensed by rotational dynamics devices, *i.e.*, ‘antennas’ based on torque^{43–57} rather than on force (translational oscillations of charges, antenna currents). However, ‘antennas’ for the radio frequency range based on rotational degrees of freedom and torque are not yet readily available. On the other hand it has been shown¹ that it is possible to use arrays consisting of a sufficient number of antennas of the conventional translational (conduction) degree of freedom type, to generate approximate OAM eigenmodes and superpositions thereof. Alternatively, one can combine such antennas with reflectors or lenses that have azimuthally dependent reflective properties³, including helicoidal parabolic antennas⁴. This makes it possible already now to use readily available analogue and digital radio techniques and technologies, including ordinary linear-momentum sensing and generating antennas, to study certain fundamental properties of OAM experimentally in the radio regime¹.

III. EXPERIMENTAL RESULTS

Since EM beams that are physically encoded with angular momentum have a particular, azimuthally dependent phase behaviour (see Table I), it is important to investigate what impact this physical fact might have, if any, on the possibilities to use OAM in radio communications based on state-of-the-art digital phase modulation protocols. For this purpose we performed an outdoor OAM radio experiment in an urban setting to test whether radio beams carrying OAM can readily transfer digitally phase-modulated information to a remote receiver under realistic conditions.

In the experiment described here, performed in Forte Marghera, Venice, Italy, 2 August 2012, we used two collinear, linearly polarized radio beams, one twisted ($m = 1$) and one untwisted ($m = 0$). As shown in Fig. 1, we generated the twisted beam with a helicoidally deformed parabolic antenna, whereas the untwisted beam was generated with a Yagi-Uda antenna, designed for the UHF S-band carrier frequency used. Because of the different signatures of the respective phase fronts of the two beams, the field vectors of a linearly polarized $m = 1$ EM beam should be in anti-phase at two points on diametrically opposite sides of the OAM phase singularity at the centre of the two aligned beams, whereas they should be in phase for an $m = 0$ beam (see Fig. 1 and Ref. 1, Fig. 2). We therefore probed the phases of the fields of the received signals at such points in a standard phase interferometric manner,

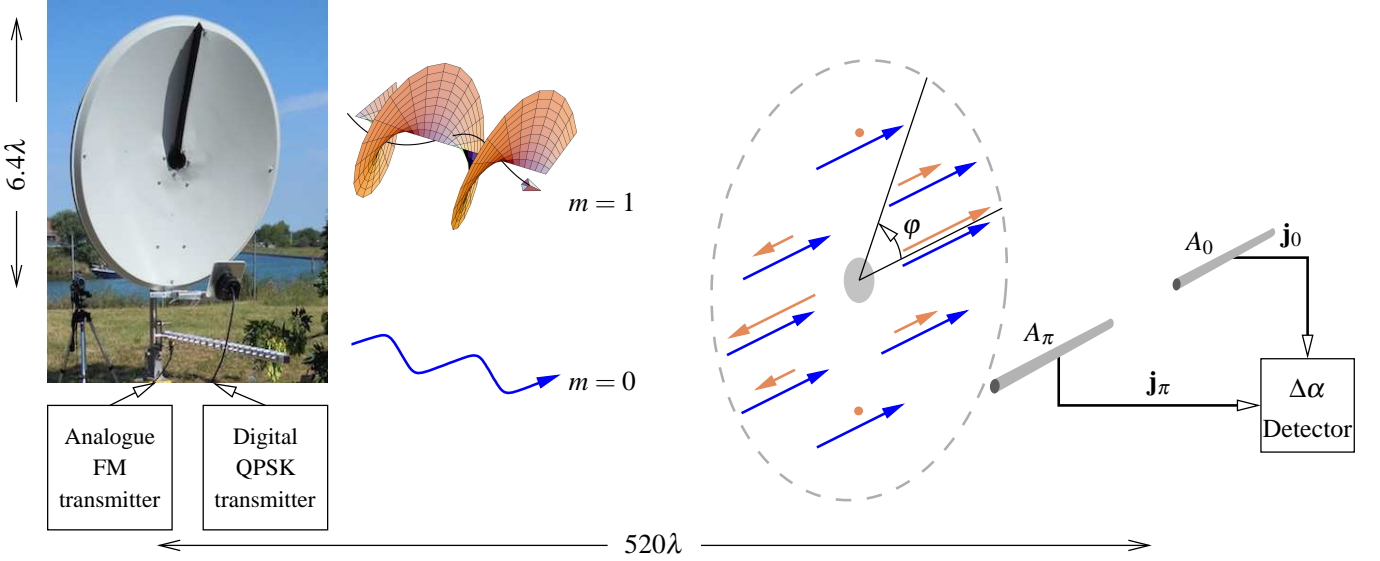


Figure 1. Schematic description of the experimental setup. The OAM $m = 1$ state (colour coded orange) was produced by a helicoidally deformed parabolic antenna of the same type as used in the experiment reported in Ref. 4. This antenna was fed by a digital QPSK transmitter operating at a carrier frequency of 2.414 GHz, transmitting live TV pictures. Horizontal linear polarization was used. The linear-momentum ($m = 0$) signal at the same carrier frequency and with the same polarization (colour coded blue) was emitted by a standard Yagi-Uda antenna, fed by an FM signal modulated with a TV test pattern. At the receiving end, at a distance of 520λ from the transmitting antennas, well into their (linear-momentum) far zones, the instantaneous EM fields of the $m = 0$ and $m = 1$ modes should be in phase on one side of the central axis (azimuthal angle $\varphi = 0$) and in anti-phase at the opposite side ($\varphi = \pi$). Therefore a simple standard linear-momentum interferometer was used in the experiment to discern between the two OAM eigenmodes. A typical phase interferometer consists of two identical antennas A_0 and A_π producing antenna current densities \mathbf{j}_0 and \mathbf{j}_π , respectively. The phase differences of these currents are measured and from these measurements the differences between the phases of the two electric field vectors are estimated. The inset illustrating the twisted beam was taken from www.gla.ac.uk/schools/physics/research/groups/optics.

using two identical antennas sensitive to the linear momentum carried by the EM field. The measurements confirmed that the phases of the received signals had the expected characteristics. This allowed us to unambiguously identify and discriminate between the $m = 0$ and $m = 1$ OAM eigenstates at the receiving end.

The transmitted $m = 1$ signal was encoded with a DVB-S protocol quadrature phase shift coding (QPSK) modulation. QPSK is a digital phase encoding technique used in many telecommunications applications today. It employs, at any given time, four different phase states $\{01, 11, 10, 00\}$ for the carrier. These four phase states correspond to $\{0, 90, 180, 270\}$ degrees of relative phase shifts, respectively. For each temporal period, the phase can change once, while the amplitude remains constant. In this way, two bits of information are conveyed within each time slot. On the same UHF S-band carrier frequency, we superimposed an untwisted ($m = 0$) 100 mW analogue frequency modulation (FM) transmission with the same horizontal polarization state as the OAM transmission. Both transmissions suffered reflections from the ground as the beams propagated from the transmitters to the 65 m (520λ) distant receivers, both placed about 1.5 m (12λ) above the reflecting ground. The QPSK constellation diagram in Fig. 3 was measured for information transfer in a 17 MHz bandwidth around the carrier frequency of 2.414 GHz in the presence of ground reflections and an interfering 100 MW FM signal, modulated with a TV test pattern, at the same carrier

frequency. As can be seen, the observed QPSK constellation diagram agrees very well with the numerically simulated one shown in Fig. 2.

The modulation error ratio (MER) of the QPSK alone was larger than 20 dB, with a bit error rate (BER) of 10^{-8} and a carrier-to-noise ratio $C/N > 15$ dB, including the effect of ground reflections.

A. Fading and reflections

Fading caused by reflections is one of the most common complications in wireless communications. Walls, ground and other objects can have a detrimental effect on a communication channel and decrease the quality of the transmission. On the other hand, reflections can also be utilized in multi-path linear-momentum communication protocols such as MIMO to increase the signal to noise ratio and to enhance the information transfer capability. So far we have not utilized any MIMO or MIMO-like techniques in our OAM radio experiments. Such experiments are pending.

With OAM states, the problem is more intricate and subtle because each reflection will introduce a parity change and OAM channel swapping from left- to right-handed twist and *vice versa*; see Table I. For the purpose of assessing the robustness of the information transfer against perturbations, we used the reflection of the waves off the ground with horizontal

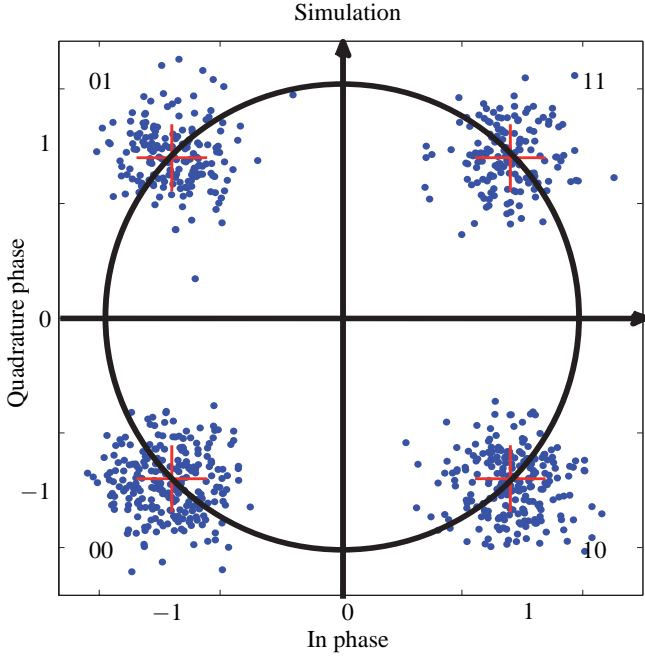


Figure 2. Numerically simulated constellation diagram for the QPSK information transfer.

polarization, since this maximizes the fading.

At the phase interferometer, the horizontally polarized OAM-carrying electromagnetic beam was received as a superposition of the $m = 1$ direct beam and the reflected beam which, because of parity inversion, was $m = -1$ charged. In order to assess the stability of the OAM mode, we gradually varied the amount of disturbance introduced by reflections by varying the inclination of the parabolic antenna transmitting the $m = 1$ mode. This allowed us to superimpose the main twisted beam and reflected beams with a reflected/transmitted beam ratio ranging from 0.25 to 0.5 of the width of the receiving beam.

Because of the fading so produced, we measured a variation of the QPSK signal from 9 to 11 dB and a resulting C/N ratio ranging from 9 to 12 dB. The MER varied in the range 10–12 dB and this guaranteed an acceptable reception of the signal.

To remove the problem of parity change, the receiver must be able to discriminate between clockwise and counterclockwise vorticities (positive and negative topological charge m). This can be achieved by using either a selective phase mask or a circular array of $2m + 1$ antennas¹.

When an FM analogue transmitter signal with the same carrier frequency was switched on, the ensuing interference on the digital, twisted signal caused the MER to vary between 10 and 12 dB, the BER from 10^{-3} to 10^{-5} , and the C/N from 9 to 15 dB, for a variation of reflected signal/signal ratio from 0.25 to 0.5.

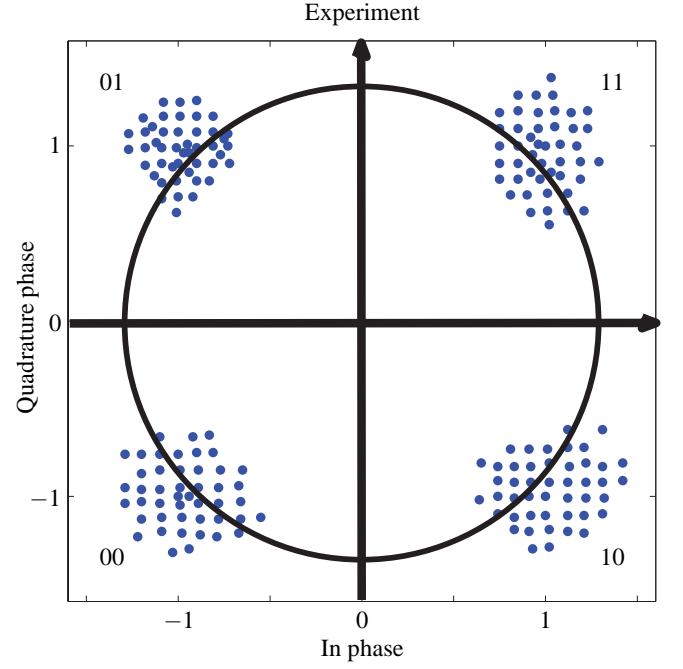


Figure 3. Constellation diagram for the QPSK information transfer as measured in the experiment in the presence of ground reflections and an interfering FM signal at the same carrier frequency.

B. Summary

Our results show that radio transmissions with OAM states are compatible and robust with respect to digital multiplexing techniques, even those based on phase coding such as phase shift keying (PSK). This is true also when the OAM signal is disturbed by the presence of a strong wide-band interfering signal on the same carrier frequency and by the presence of ground reflections. The importance of our findings lies in the fact that PSK protocols are at the core of the digital modulation techniques used in modern telecommunications and broadcasting and in many other of today's wireless scenarios. This offers the convenience of back-compatibility between the new angular momentum and current linear momentum radio methods.

Our experimental results are in full agreement with numerical simulations performed. The maximum separation was 30 dB whereas for vertical polarization we estimate it to be up to 50 dB. This clearly shows that OAM can be used to increase the transmission capacity of our common-use devices, allowing multiple services and users to share the same frequency band.

We consider our experimental verification of the feasibility of using OAM radio in communications applications using phase modulation a significant leap forward, and a pivotal step toward the implementation of novel radio concepts, applications and protocols.

IV. METHODS

The digital transmitter used for the twisted ($m = 1$) mode, a Microwave Link QPSK DVB-S transmitter for the 2.4 GHz band, was tuned to 2.414 GHz (free-space wavelength $\lambda = 12.49$ cm). It transmitted live encoded video images at a rate of 11.5 Megasymbols/s. For correction purposes, we used a forward error correction of the FEC=3/4 type, meaning that after three bits transmitted, a fourth bit was added. This transmitter was connected to an 80 cm (6.4λ) diameter twisted parabolic antenna with a four elements patch feeder producing a twisted ($m = 1$) OAM beam.

In addition, an 1 W analogue FM transmitter, fit with a 10 dB attenuator on the output, was used for transmitting a colour-bar TV test pattern on the same frequency and along the same path. The antenna used for this transmitter was a commercial-off-the-shelf (COTS) 16–20 dBi Yagi-Uda antenna, producing an untwisted ($m = 0$) beam.

The two receiving antennas, used in a conventional phase interferometric setup to measure the phase of the EM field, were two identical 26 cm (2.1λ) diameter, 16 dBi backfire antennas connected together through a signal splitter/combiner. A phase tuner, in the form of a silver slit waveguide coupled to a Selenia signal circulator, was inserted into one of the interferometer arms. By moving the cursor in the slit waveguide, we retarded the signal received by one of the two interferometer antennas relative to the other.

The signals collected by the interferometer were split up into three different receiver chains: (1) a digital DVB-S digital chain with a QPSK constellation tester, (2) a spectrum analyzer chain for measuring and testing, and (3) an analogue frequency modulation (FM) chain. In the latter chain we inserted a high-pass filter to block out the direct current (DC) and audio frequency components.

The received signal was routed to an analyzer and/or to a 3-way power splitter, where it was down-converted with a local oscillator (LO) of 900 MHz to 1.514 GHz and split into three different lines: (1) DVB-S, (2) analogue FM, and (3) the analyzer again.

The average background noise power in a 100 MHz bandwidth was measured at -93 dBm, peaking at -85.6 dBm at the centre frequency. The power of the received FM signal was measured by inserting the spectrum analyzer in the reception line and was found to be -68.95 dBm in a 17 MHz wide transmission band.

REFERENCES

- ¹Thidé, B. *et al.* Utilization of photon orbital angular momentum in the low-frequency radio domain. *Phys. Rev. Lett.* **99**, 087701(4) (2007).
- ²Tamburini, F., Thidé, B., Molina-Terriza, G. & Anzolin, G. Twisting of light around rotating black holes. *Nature Phys.* **7**, 195–197 (2011).
- ³Tamburini, F., Mari, E., Thidé, B., Barbieri, C. & Romanato, F. Experimental verification of photon angular momentum and vorticity with radio techniques. *Appl. Phys. Lett.* **99**, 204102 (2011).
- ⁴Tamburini, F. *et al.* Encoding many channels on the same frequency through radio vorticity: first experimental test. *New J. Phys.* **14**, 03301 (2012).
- ⁵Tamburini, F. *et al.* Reply to comment on ‘Encoding many channels on the same frequency through radio vorticity: first experimental test’. *New J. Phys.* **14**, 118002 (2012).
- ⁶Heitler, W. *The Quantum Theory of Radiation*. The International Series of Monographs on Physics (Clarendon Press, Oxford, UK, 1954), 3 edn. Appendix 1.
- ⁷Bogolyubov, N. N. & Shirkov, D. V. *Introduction to the Theory of Quantized Fields*, vol. III of *Interscience Monographs in Physics and Astronomy*, chap. 2 (Interscience, New York, NY, USA, 1959).
- ⁸Messiah, A. *Quantum Mechanics*, chap. XXI, Sect. 23 (North-Holland, Amsterdam, NL, 1970).
- ⁹Eyges, L. *The Classical Electromagnetic Field*, chap. 11 (Dover Publications, New York, NY, USA, 1972).
- ¹⁰Berestetskii, V. B., Lifshitz, E. M. & Pitaevskii, L. P. *Quantum Electrodynamics*, vol. 4 of *Course of Theoretical Physics*, chap. 1 (Pergamon Press, Oxford, UK, 1989), 2 edn.
- ¹¹Ribarič, M. & Šušteršič, L. *Conservation Laws and Open Questions of Classical Electrodynamics* (World Scientific, Singapore, New Jersey, London, Hong Kong, 1990).
- ¹²Mendel, L. & Wolf, E. *Optical Coherence and Quantum Optics*, chap. 10 (Cambridge University Press, New York, NY, USA, 1995).
- ¹³Cohen-Tannoudji, C., Dupont-Roc, J. & Grynberg, G. *Photons and Atoms: Introduction to Quantum Electrodynamics*, chap. 1 (Wiley, New York, NY, USA, 1997).
- ¹⁴Schwinger, J., DeRaad, L. L., Jr., Milton, K. A. & Tsai, W. *Classical Electrodynamics*, chap. 3 (Perseus Books, Reading, MA, USA, 1998).
- ¹⁵Jackson, J. D. *Classical Electrodynamics*, chap. 7 and 12 (Wiley, New York, 1998), 3 edn.
- ¹⁶Allen, L., Barnett, S. M. & Padgett, M. J. *Optical Angular Momentum* (IOP, Bristol, UK, 2003).
- ¹⁷Rohrlich, F. *Classical Charged Particles*, chap. 7 (World Scientific, Singapore, 2007), 3 edn.
- ¹⁸Andrews, D. L. *Structured Light and Its Applications: An Introduction to Phase-Structured Beams and Nanoscale Optical Forces* (Academic Press, Amsterdam, NL, 2008).
- ¹⁹Torres, J. P. & Torner, L. *Twisted Photons: Applications of Light With Orbital Angular Momentum* (Wiley-Vch Verlag, John Wiley and Sons, Weinheim, DE, 2011).
- ²⁰Yao, A. M. & Padgett, M. J. Orbital angular momentum: origins, behavior and applications. *Adv. Opt. Photon.* **3**, 161–204 (2011).
- ²¹Thidé, B. *Electromagnetic Field Theory*, chap. 4 (Dover Publications, Inc., Mineola, NY, USA, 2011), 2nd edn. URL <http://www.plasma.uu.se/CED/Book>. (In press).
- ²²Franke-Arnold, S., Allen, L. & Padgett, M. Advances in optical angular momentum. *Laser & Photon. Rev.* **2**, 299–313 (2008).
- ²³Thidé, B., Elias, N. M., II, Tamburini, F., Mohammadi, S. M. & Mendonça, J. T. Applications of electromagnetic OAM in astrophysics and space physics studies. In Torres, J. P. & Torner, L. (eds.) *Twisted Photons: Applications of Light With Orbital Angular Momentum*, chap. 9, 155–178 (Wiley-Vch Verlag, Weinheim, DE, 2011).
- ²⁴Gibson, G. *et al.* Free-space information transfer using light beams carrying orbital angular momentum. *Opt. Express* **12**, 5448–5456 (2004).
- ²⁵Čelechovský, R. & Bouchal, Z. Optical implementation of the vortex information channel. *New J. Phys.* **9**, 328 (2007).
- ²⁶Barreiro, J. T., Wei, T.-C. & Kwiat, P. W. Beating the channel capacity limit for linear photonic superdense coding. *Nature Phys.* **4**, 282–286 (2008).
- ²⁷Pors, J. B. *et al.* Shannon dimensionality of quantum channels and its application to photon entanglement. *Phys. Rev. Lett.* **101**, 120502 (2008).
- ²⁸Martelli, P., Gatto, A., Boffi, P. & Martinelli, M. Free-space optical transmission with orbital angular momentum division multiplexing. *Electron. Lett.* **47**, 972–973 (2011).
- ²⁹Kumar, A., Prabhakar, S., Vaity, P. & Singh, R. P. Information content of optical vortex fields. *Opt. Lett.* **36**, 1161–1163 (2011).
- ³⁰Wang, J. *et al.* Terabit free-space data transmission employing orbital angular momentum multiplexing. *Nature Photon.* **6**, 488–496 (2012).
- ³¹Belinfante, F. J. On the current and the density of the electric charge, the energy, the linear momentum and the angular momentum of arbitrary fields. *Physica* **7**, 449–474 (1940). URL <http://www.sciencedirect.com/science/article/B6X42-4CB7521-3D/2/9949>
- ³²Soper, D. E. *Classical Field Theory*, chap. 9 (John Wiley & Sons, Inc., New York, NY, USA, 1976).
- ³³Truesdell, C. *Essays in the History of Mechanics*, chap. V (Springer-Verlag, Berlin, Heidelberg, New York, 1968).
- ³⁴Berry, M. V. Optical vortices evolving from helicoidal integer and fractional phase steps. *J. Opt. A: Pure Appl. Opt.* **6**, 259–268 (2004).
- ³⁵Torner, L., Torres, J. P. & Carrasco, S. Digital spiral imaging. *Opt. Express* **13**, 873–881 (2005).
- ³⁶Molina-Terriza, G., Torres, J. P. & Torner, L. Management of the angular momentum of light: Preparation of photons in multidimensional vector states of angular momentum. *Phys. Rev. Lett.* **88**, 013601(4) (2002).
- ³⁷Litchinitser, N. M. Structured light meets structured matter. *Science* **337**, 1054–1055 (2012).
- ³⁸Mair, A., Vaziri, A., Weihs, G. & Zeilinger, A. Entanglement of the orbital

- angular momentum states of photons. *Nature* **412**, 313–316 (2001).
- ³⁹Abraham, M. Der Drehimpuls des Lichtes. *Physik. Zeitschr.* **XV**, 914–918 (1914).
- ⁴⁰Thidé, B., Lindberg, J., Then, H. & Tamburini, F. Linear and angular momentum of electromagnetic fields generated by an arbitrary distribution of charge and current densities at rest (2010). URL <http://arxiv.org/abs/1001.0954>. [physics.class-ph]:1001.0954.
- ⁴¹Eddington, A. S. *The Nature of the Physical World* (Kessinger Publishing, 2010).
- ⁴²Jackson, J. D. *Classical Electrodynamics* (Wiley & Sons, New York, NY, USA, 1998), 3 edn.
- ⁴³Then, H. & Thidé, B. Mechanical properties of the radio frequency field emitted by an antenna array (2008). URL <http://arxiv.org/abs/0803.0200>. [physics.class-ph]:0803.0200.
- ⁴⁴Beth, R. A. Direct detection of the angular momentum of light. *Phys. Rev.* **48**, 471 (1935).
Beth, R. A. Mechanical detection and measurement of the angular momentum of light. *Phys. Rev.* **50**, 115–125 (1936).
- ⁴⁵Holbourn, A. H. S. Angular momentum of circularly polarised light. *Nature* **137**, 31–31 (1936).
- ⁴⁶Carrara, N. Torque and angular momentum of centimetre electromagnetic waves. *Nature* **164**, 882–884 (1949).
- ⁴⁷Allen, P. J. A radiation torque experiment. *Am. J. Phys.* **34**, 1185–1192 (1966).
- ⁴⁸Carusotto, S., Fornaca, G. & Polacco, E. Radiation beats and rotating systems. *Nuov. Cim.* **53**, 87–97 (1968).
- ⁴⁹Chang, S. & Lee, S. S. Optical torque exerted on a homogeneous sphere levitated in the circularly polarized fundamental-mode laser beam. *J. Opt. Soc. Am. B* **2**, 1853–1860 (1985).
- ⁵⁰Vul’fson, K. S. Angular momentum of electromagnetic waves. *Sov. Phys. Usp.* **30**, 667–674 (1987).
- ⁵¹Kristensen, M., Beijersbergen, M. W. & Woerdman, J. P. Angular momentum and spin-orbit coupling for microwave photons. *Opt. Commun.* **104**, 229–233 (1994).
- ⁵²He, H., Friese, M. E. J., Heckenberg, N. R. & Rubinsztein-Dunlop, H. Direct observation of transfer of angular momentum to absorptive particles from a laser beam with a phase singularity. *Phys. Rev. Lett.* **75**, 826–829 (1995).
- ⁵³Friese, M. E. J., Enger, J., Rubinsztein-Dunlop, H. & Heckenberg, N. R. Optical angular-momentum transfer to trapped absorbing particles. *Phys. Rev. A* **54**, 1593–1596 (1996).
- ⁵⁴Helmerson, K. *et al.* Vortices and persistent currents: Rotating a Bose-Einstein condensate using photons with orbital angular momentum. *Topologica* **2**, 002 (2009).
- ⁵⁵Padgett, M. & Bowman, R. Tweezers with a twist. *Nature Phys.* **5**, 343–348 (2011).
- ⁵⁶Ramanathan, A. *et al.* Superflow in a toroidal Bose-Einstein condensate: An atom circuit with a tunable weak link. *Phys. Rev. Lett.* **106**, 130401 (2011). URL <http://link.aps.org/doi/10.1103/PhysRevLett.106.130401>.
- ⁵⁷Elias, N. M., II. Photon orbital angular momentum and torque metrics for single telescopes and interferometers. *Astron. Astrophys.* **541**, A101 (2012).

ACKNOWLEDGMENTS

We gratefully acknowledge Andrea Bonifacio and Marco Polo System for the help and permission to use the experiment location Forte Marghera, and Tamara Vidali and Enzo Bon for their help and support during the experiment. B.T. was financially supported by the Swedish National Space Board (SNSB).